Real-time Prediction of Leg Joint Kinematics during Steady-State Walking and Task Transitions*

Louis Devillez[1,3] and Renaud Ronsse[1,2]

***Abstract*— Amputations and other impairments heavily impact human locomotion. To compensate for these disabilities, advanced devices such as active orthoses and prostheses are being developed with the aim of restoring locomotor function. To achieve this goal, the control of such technologies has been identified as a key research challenge. A reference kinematic profile for the affected or missing joints is often useful for device control. This paper introduces a novel method for estimating reference kinematics of leg joints from kinematic signals of the contralateral leg. This method leverages fusion of two different estimators – i.e. Complementary Limb Motion Estimation and Adaptive Oscillators – which are combined through the use of a logistic function. The method is then applied to estimate the kinematics of a hip joint, and the performance is compared with that of each individual estimator during walking. The correlation between the estimated signal and the ground truth is assessed on a cycle-by-cycle basis. During transitions, our new method behaves similarly to Complementary Limb Motion Estimation. After a few cycles, the method shifts towards Adaptive Oscillators to achieve a better correlation during quasi-steady-state locomotion.**

I. Introduction

There are many neuromusculoskeletal disorders impacting lower limb functions. Examples include Parkinson's disease, stroke, or amputation, and each of them leads to serious locomotion disabilities. Advanced technologies have been developed to alleviate the effects of these disorders, such as powered orthoses [1], [2] or prostheses [3], [4]. A key challenge that remains to be solved is the control of such technologies. A particularly emerging approach consists in governing the device behavior through bio-inspired control principles, mainly through descending activation patterns, feedback-driven reflexes, and/or motor primitives [5]. Implementation of such control can be divided into two key steps. First, reference kinematics of affected joints need to be generated. Then, the device behavior is regulated as a function of these reference kinematics, either through a stiff PID controller [6], or by computing assist-as-needed force profiles in an impedance-based controller [7]. Finite-state machines can be used to sequence the controller behavior into a series of distinct phases synchronized with events — such as heel strike — to modulate gains or combine different control modes [8], [9].

In this paper, the focus is on the first step, i.e. generation of relevant reference kinematics. Since the corresponding joint

*This work was supported by the Belgian F.R.S.-FNRS (Aspirant #40011487 awarded to LD)

[1]Institute of Mechanics, Materials and Civil Engineering and Louvain Bionics, UCLouvain, 1348 Louvain-la-Neuve, Belgium

[2]Institute of Neuroscience, UCLouvain, 1200 Brussels, Belgium

[3]`louis.devillez@uclouvain.be`

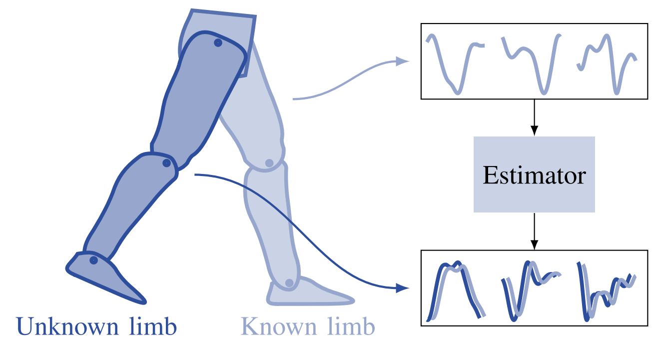

Fig. 1. Schematic representation of the problem statement. By measuring the kinematic signals of one leg, we aim at predicting the kinematics of at least one joint of the contralateral leg.

is missing or no longer functional, its reference kinematics need to be estimated, for instance by measuring signals on the contralateral leg. Ideally, this reference kinematics should also adapt as a function of the executed task: leg joints do not follow the same pattern during overground walking and stair ascending/descending, and even during walking at two different speeds. These statements are particularly relevant for proximal joints, since they govern the whole leg rhythmicity [10]. For example, in the case of hip disarticulation, i.e. amputation of a whole leg, the reference kinematics of the hip prosthesis module could only be estimated from signals measured on the rest of the body [11].

Human locomotion is a combination of rhythmic and discrete movements [12]. Walking and ascending stairs are examples of rhythmic movements — at least during their steady-state segments — while the transition from standing to walking or sitting are discrete movements. A large proportion of controllers for assistive locomotion devices rely on phase-based methods, i.e., real-time estimation of a continuously evolving gait phase between 0 % and 100 % [13] to generate reference kinematics. This implies that they only work during (quasi-)rhythmic tasks. For example, [14] used precomputed signals as reference kinematics, that varied with respect to the estimated gait phase. In echo control, the kinematic profile of one joint is recorded and replayed with some time delay to serve as a reference for the contralateral joint [15]. Adaptive Oscillators (AO) are dynamical systems capable of synchronizing with a quasi-periodic input by learning its features in state variables [16]. Since these methods require rhythmicity, they are not well adapted to discrete transitions. Other methods, such as Complementary Limb Motion Estimation (CLME), do not leverage the intrinsic rhythmicity of locomotion in their working principle. CLME infers the intended motion of the affected joints from the motion of the residual joints [17]. This method can handle transitions but requires specific parameter tuning for each task and potentially even for each user.

The methodology presented in this paper combines two methods, i.e. AO and CLME, in order to leverage their respective benefits. We strive to develop an estimator adapted to both discrete and rhythmic segments of walking, i.e. giving precedence to AO during rhythmic segments, and to CLME during discrete transitions. Additionally, this method can reduce the need for gain tuning. The article is structured as follows: Section II presents the problem statement. Section III overviews the algorithms of CLME and AO in detail. The mechanism to combine both methods is described in Section IV. Section V applies this combined estimator to our target application, i.e. estimating the kinematics of a missing hip joint. Results are compared and analyzed in Section VI. The paper ends with a discussion and a conclusion.

II. Problem statement

The problem addressed in the present paper consists in estimating in real-time the joint kinematics of one leg from measurements of kinematic signals taken from the other leg. A schematic representation is depicted in Fig. 1. Let $\boldsymbol{q}$ be a time-dependent vector with $3M$ components containing kinematic signals of M leg joints, such that for each joint i:

- $q_{3(i-1)+1}$ is the joint position
- $q_{3(i-1)+2}$ is the joint velocity
- $q_{3(i-1)+3}$ is the joint acceleration

The problem can thus be expressed as finding a function f such that:

$$\boldsymbol{q}_U[t] = f(\boldsymbol{q}_K[t]) \tag{1}$$

The subscripts K and U are used to denote the known limb and the unknown one.

III. Related work

In this section, we overview two existing methodologies providing a particular implementation of the function f. First, CLME augmented with a Kalman filter is presented; then AO are introduced.

A. Complementary limb motion estimation

CLME was developed by Vallery and colleagues in [17]–[20]. The principle behind this method is to leverage interjoint coordination [21] and, consequently, to find the best linear combination of known joint kinematic variables (position, velocity, and/or acceleration) to estimate similar variables of another joint.

To construct a CLME, data from both known and unknown joints are required. Moreover, this framework does not require to specify which kinematic variables are used to compose vectors $\boldsymbol{q}_U$ and $\boldsymbol{q}_K$ since it can be implemented with any combination of position, velocity, and acceleration signals.

The first step consists in normalizing the variables, i.e. computing normalized vectors $\boldsymbol{x}$ as:

$$\boldsymbol{S}_i = \mathrm{diag}\left(\mathrm{var}(\boldsymbol{q}_i)\right) \tag{2}$$

$$\boldsymbol{x}_i = \boldsymbol{S}_i^{-1}\left(\boldsymbol{q}_i - \bar{\boldsymbol{q}}_i\right) \tag{3}$$

with $\mathrm{var}(\boldsymbol{q}_i)$ being the variance and $\bar{\boldsymbol{q}}_i$ the mean of $\boldsymbol{q}_i$, and the subscript i denoting both U and K. The best estimator is defined as the matrix $\boldsymbol{C}$ such that the expected error between the normalized vector of the unknown joint and the estimation is minimized, i.e.:

$$\mathrm{argmin}\left(\sum(||\boldsymbol{x}_U - \boldsymbol{C}\boldsymbol{x}_K||)\right) \tag{4}$$

Importantly, since this problem is linear, it has an exact solution, that can be computed as:

$$\boldsymbol{C}_{\text{opt}} = \left(\mathrm{cov}^{-1}(\boldsymbol{x}_K, \boldsymbol{x}_K) * \mathrm{cov}(\boldsymbol{x}_K, \boldsymbol{x}_U)\right)^T \tag{5}$$

with $\mathrm{cov}(\cdot,\cdot)$ denoting the covariance function. An estimator of the unknown joint kinematics can then be constructed as:

$$\boldsymbol{q}_U^{\text{CLME}} = \boldsymbol{A}\boldsymbol{q}_K + \boldsymbol{b} \tag{6}$$

$$\boldsymbol{A} = \boldsymbol{S}_U\boldsymbol{C}\boldsymbol{S}_K^{-1} \tag{7}$$

$$\boldsymbol{b} = \boldsymbol{A}\bar{\boldsymbol{q}}_K + \bar{\boldsymbol{q}}_U \tag{8}$$

This approach computes estimates of the kinematic variables independently of each other, i.e. without accounting for the fact that one might be the derivative of another. In other words, following the problem statement, it does not guarantee that the derivative of $q_{3(i-1)+1}$ is equal to $q_{3(i-1)+2}$ and that the derivative of $q_{3(i-1)+2}$ is equal to $q_{3(i-1)+3}$.

However, there are many reasons why satisfying these constraints between position, velocity, and/or acceleration is essential. For instance, if the position estimate is used as a reference signal for a controller, its dynamics can benefit greatly from having an estimate of the reference velocity, as long as it is the actual derivative of the position [22].

To solve this problem, this correlation-based CLME measurement can be coupled with a model-based prediction that takes into account the derivative relationship between variables. This can be achieved by coupling a Kalman filter [17], thus combining a predictor based on an internal model with a series of integrators, to the CLME-based estimation [23]. Therefore, we define the following variables:

- $\boldsymbol{q}_U^*$: the prediction from the internal model of the filter
- $\boldsymbol{q}_U^{\text{KF}}$: the output from the Kalman filter, combining the model-based prediction and CLME-based estimation
- $\boldsymbol{K}$: the Kalman gain matrix

The internal model estimate is expressed as a chain of Euler-explicit integrators, i.e.:

$$\boldsymbol{q}_U^*[t+1] = \begin{bmatrix} \boldsymbol{F} & & \\ & \ddots & \\ & & \boldsymbol{F} \end{bmatrix} \boldsymbol{q}_U^{\text{KF}}[t] \tag{9}$$

where

$$\boldsymbol{F} = \begin{bmatrix} 1 & \Delta t & 0 \\ 0 & 1 & \Delta t \\ 0 & 0 & 1 \end{bmatrix} \tag{10}$$

The output of the whole filter is then obtained as:

$$\boldsymbol{q}_U^{\mathrm{KF}}[t+1] = \boldsymbol{q}_U^{*}[t+1] + \boldsymbol{K}\left(\boldsymbol{q}_U^{\mathrm{CLME}}[t] - \boldsymbol{q}_U^{*}[t]\right) \tag{11}$$

The principle of a Kalman filter is to find the best gain matrix $\boldsymbol{K}$ that minimizes the error of the combined estimates. Several references explain how to compute $\boldsymbol{K}$, as a function of the covariance of the process noise (here the variance of the acceleration, i.e. $\mathrm{var}\left(q_{U,3(i-1)+3}\right)$) and the observation noise (here, the variance of the measurement error, i.e. $\mathrm{var}\left(q_{U,3(i-1)+1}^{\mathrm{CLME}} - q_{U,3(i-1)+1}\right)$) [24].

B. Adaptive oscillators

Any periodic signal can be decomposed into an infinite sum of sinusoidal signals, as captured by Fourier's theorem. An estimate of this signal can be constructed by truncating this sum to its first N terms. Such an estimation can be applied to the position of the known leg and is thus expressed as:

$$q_{K,3(i-1)+1}^{\mathrm{AO}}(t) = \alpha_0 + \sum_{j=1}^{N} \alpha_j \sin\left(\phi_j(t)\right) \tag{12}$$

$$\dot{\phi}_j(t) = j\omega \tag{13}$$

with the following parameters: α_0 the offset, α_j the amplitude of the j-th harmonic, ω the frequency of the fundamental harmonic, and ϕ_j the phase of the j-th harmonic.

AO are a mathematical tool specifically developed in order to estimate these parameters [25]. The estimation error, ϵ is computed as the difference between the periodic signal to be estimated and its estimation. Here we assume the signal to be estimated is the measured joint angular position of the known leg, i.e.:

$$\epsilon(t) = q_{K,3(i-1)+1}(t) - q_{K,3(i-1)+1}^{\mathrm{AO}}(t) \tag{14}$$

The dynamics governing the learning of the estimation state variables are given as follows:

$$\dot{\alpha}_0(t) = \epsilon(t)\ \eta \tag{15}$$

$$\dot{\alpha}_j(t) = \epsilon(t)\ \eta \sin\left(\phi_j(t)\right) \tag{16}$$

$$\dot{\omega}(t) = \epsilon(t)\ \nu_\omega \frac{\cos\left(\phi_1(t)\right)}{\sum_{j=1}^{N} \alpha_j(t)} \tag{17}$$

$$\dot{\phi}_j(t) = \epsilon(t)\ \nu_\phi \frac{\cos\left(\phi_j(t)\right)}{\sum_{j=1}^{N} \alpha_j(t)} + j\omega(t) \tag{18}$$

with η, ν_ω and ν_ϕ being the learning gains for, respectively, the amplitude, frequency and phase. Note that the state equations (15)-(18) should be discretized in order to be solved in real-time. This can be done through classical explicit integration schemes like Euler or Runge-Kutta. In [16], a method to tune the learning gains gave the following rules:

$$\eta = \frac{2}{\tau_\alpha} \qquad \nu_\omega = \frac{20}{\tau_\omega^2} \qquad \nu_\phi = \frac{22}{\tau_\omega} \tag{19}$$

with τ_α and τ_ω being the time constants of the amplitude and frequency dynamics, respectively.

Assuming that both legs are in antiphase during walking, the estimation of the unknown leg can be built based on the state variables learned from the known leg, yet with an extra phase shift of $j\pi$. The estimation of the unknown angular position can then be expressed as:

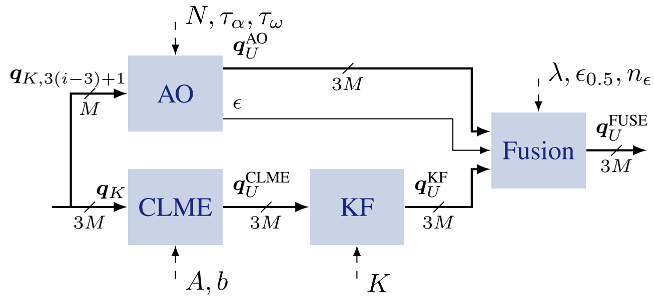

Fig. 2. Block diagram of the various components of the fused estimator. Each block has its own parameters, represented by the vertical arrows. The input of both CLME and AO are kinematics signals. The CLME output is filtered with a Kalman filter (KF). Fusion of both estimators is governed by the AO error ϵ.

$$q_{U,3(i-1)+1}^{\mathrm{AO}}(t) = \alpha_0(t) + \sum_{j=1}^{N} \alpha_j(t) \sin\left(\phi_j(t) + j\pi\right) \tag{20}$$

The velocity and acceleration can be obtained by analytically differentiating (20), i.e.:

$$q_{U,3(i-1)+2}^{\mathrm{AO}}(t) = \sum_{j=1}^{N} \alpha_j(t) j\omega(t) \cos\left(\phi_j(t) + j\pi\right) \tag{21}$$

$$q_{U,3(i-1)+3}^{\mathrm{AO}}(t) = -\sum_{j=1}^{N} \alpha_j(t) j^2 \omega(t)^2 \sin\left(\phi_j(t) + j\pi\right) \tag{22}$$

Since AO build a kind of real-time Fourier series, it only works during (quasi-)rhythmic movements, i.e. steady-state walking. During transients, its performance degenerates to that of a low-pass filter.

IV. Fusing the Estimators

In the previous section, we introduced CLME and AO, two methods to estimate the unknown leg kinematics from the known one. In this section, both estimators are fused together to obtain a more robust estimation of the unknown side. Fig. 2 illustrates the relationship between the different blocks.

Both methods have their advantages and disadvantages. CLME is time-invariant and provides a time-independent optimal estimation, in the least-squares sense. However, the quality of this estimation depends on the dataset on which the gains have been optimized and does not exactly satisfy relationships between position, velocity, and acceleration signals. AO can provide an estimation that is exactly in antiphase with respect to the known leg and that satisfies relationships between kinematic derivatives. However, it is governed by its intrinsic dynamics and thus needs time to reach a new (quasi) steady-state after each transition. As a consequence, it is preferable to use the estimation from CLME during transient phases, and to give more weight to the estimation provided by AO once steady-state locomotion has been reached.

A fixed weighted average between both estimators would not take into account the temporal dynamics of the AO-based estimation. Yet, the quality of this AO-based estimation is directly provided by the error signal ϵ. For large ϵ, when the estimation does not match the measurement, state variables evolve rapidly (15-18), indicating that AO have not converged. In contrast, small ϵ indicates a slow evolution of state variables, capturing that AO have converged.

In order to hide high-frequency variations in both the measured signal and its estimate, we chose to use the moving average of ϵ, denoted, ϵ_{MA}, as the convergence metric of AO. Its window size is denoted by n_ϵ. The weight that should be given to the estimation provided by AO is then defined by the following logistic function, bounded between 0 and 1:

$$W(\bar{\epsilon}) = 1 - \frac{1}{1 + \exp\left(\lambda\left(\epsilon_{0.5} - \epsilon_{\mathrm{MA}}\right)\right)} \tag{23}$$

with $\epsilon_{0.5}$ being a parameter equal to the value of ϵ_{MA} corresponding to a weight of 0.5, and λ being another parameter capturing the function steepness. The nonlinear profile of (23) allows a rapid shift between CLME and AO. The output of the fused estimator is eventually computed as:

$$\boldsymbol{q}_U^{\mathrm{FUSE}} = W(\epsilon_{\mathrm{MA}}) \cdot \boldsymbol{q}_U^{\mathrm{AO}} + (1 - W(\epsilon_{\mathrm{MA}})) \cdot \boldsymbol{q}_U^{\mathrm{CLME}} \tag{24}$$

V. Application for an Active Hip Prosthesis

The previous section showed how to fuse CLME- and AO-based estimations into a single estimate, giving more weight to AO when it has converged, i.e. during steady-state locomotion. In this section, this algorithm is applied to estimate the position and velocity of a hip joint. These estimates could be used directly to control a hip prosthesis, like the one we developed in [11]. In the remainder of this section, the position of the unknown hip will be denoted θ and its velocity $\dot{\theta}$.

A. Dataset

Two pre-existing datasets were used to train, test and evaluate the estimators. The position and velocity of both legs were extracted as well as their decomposition into gait cycles. The first dataset is taken from [26] and contains data from 12 subjects performing different cyclic or non-cyclic locomotion-related tasks. Only walking trials with speeds ranging from $0.6\,\mathrm{m\,s^{-1}}$ to $1.8\,\mathrm{m\,s^{-1}}$ were kept for analysis. The second dataset is taken from [27] and contains data from 22 subjects who also performing different locomotion tasks. Only the level-ground and treadmill trials were kept for all subjects, with walking speeds ranging from $0.5\,\mathrm{m\,s^{-1}}$ to $1.85\,\mathrm{m\,s^{-1}}$. Trials with fewer than 5 cycles were excluded. This resulted in a total of 329 trials and 1,974 cycles. We arbitrarily chose the right leg as the known leg and the left leg as the unknown leg for each trial.

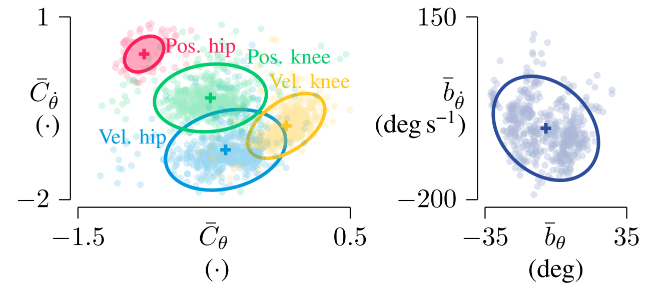

Fig. 3. Normalized gains of CLME trained on all available trials. Left: $\boldsymbol{C}$ matrix; right: $\boldsymbol{b}$ vector. The color represents the different input signals of CLME and each axis captures its magnitude for estimating both the position and velocity of the hip. Ellipses capture the normalized distribution of these points.

B. Generic CLME implementation

The CLME implementation is very similar to that of [17], where the authors showed that using acceleration signals to estimate position and velocity was of little interest. Therefore, we also decided to use only the position and velocity signals of the known leg to build the estimate. Furthermore, only hip and knee signals are used and not ankle ones, with the aim of keeping requirements for body instrumentation as low as possible, given our target application.

Data from both the known and unknown joints are required to compute the gains of CLME. Using data from the same user for both learning and estimation leads to an individualized CLME, i.e. with user-dependent gains $\boldsymbol{A}$ and $\boldsymbol{b}$. This yields the optimal CLME that can be designed for a given individual and task. However it is not always possible to have access to these data for each and every user. For instance, no data exist for the unknown joint kinematics of an individual with an amputation.

On the other hand, it is possible to use generic gains for CLME, providing a kind of “one-size-fits-all” estimator. This degrades individual estimations but removes the need for learning data for each user. To compute these generic gains, matrix $\boldsymbol{A}$ (7) and $\boldsymbol{b}$ (8) are averaged over all available trials. A representation of the distribution of the best individual gains, along with their mean value, is shown in Fig. 3. Note that the $\boldsymbol{C}$ matrix is displayed in Fig. 3 instead of the $\boldsymbol{A}$ matrix, as it captures normalized gains. As pictured in Fig. 3, each indiviual gain is distributed in signal-dependent dense clusters. This suggests that averaging may be a valid approach, at least when it is not possible to compute individualized gains.

For the used datasets, numerical values for $\bar{\boldsymbol{A}}$ and $\bar{\boldsymbol{b}}$ are the following:

$$\bar{\boldsymbol{A}} = \begin{pmatrix} -0.987 & -0.063\,\mathrm{s} & -0.439 & 0.003\,\mathrm{s} \\ 2.47\,\mathrm{s^{-1}} & -1.15 & -1.79\,\mathrm{s^{-1}} & -0.473 \end{pmatrix} \tag{25}$$

$$\bar{\boldsymbol{b}} = \begin{pmatrix} -4.95\,\mathrm{deg} \\ -63.3\,\mathrm{deg\,s^{-1}} \end{pmatrix} \tag{26}$$

The Kalman gain matrix is also averaged over all trials, and

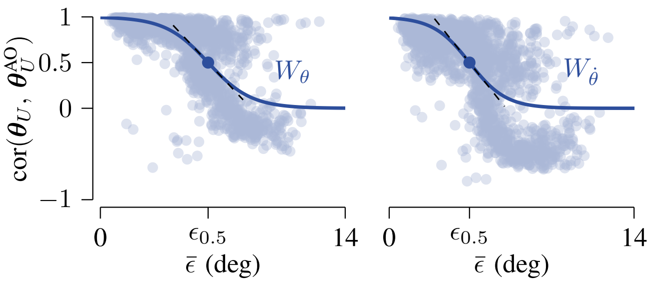

Fig. 4. Correlation between the AO-based estimation and ground-truth signals from the dataset, as a function of the time-averaged AO error $\bar{\epsilon}$, for the position (left) and velocity (right) signals. Each dot represents one walking cycle for the datasets. The solid lines represent the best possible fit of the weighting function (23), eventually used as weight given to the AO-based estimation. The dashed line captures the slope of the logistic function at $(\epsilon_{0.5}, 0.5)$.

we obtained the following optimal gains:

$$\bar{\boldsymbol{K}} = \begin{pmatrix} 0.049 & 0.004\,\mathrm{s} \\ 0.179\,\mathrm{s}^{-1} & 0.446 \end{pmatrix} \tag{27}$$

C. AO implementation

AO parameters were selected as follows: $N = 3$, $\tau_\alpha = \tau_\omega = 3\,\mathrm{s}$. At the beginning of each trial, the initial parameters of AO were set to the following values: $\alpha_0 = \alpha_i = 1\,\mathrm{deg}$, $\omega = 5\,\mathrm{rad\,s^{-1}}$ and $\phi_i = 0\,\mathrm{rad}$.

A useful pragmatic addition to the generic AO is to prevent the learned frequency ω to go below a certain threshold. This facilitates convergence during steady-state locomotion. Here, we set a threshold to 0.3 Hz, i.e. well below a typical walking frequency.

D. Merging function

In the fused estimator, a window size $n_\epsilon = 100$ was used, which corresponds to a time frame of 0.5 s, given the signal sampling rate. The parameters of the logistic function (23), i.e. λ and $\epsilon_{0.5}$, were fitted using values from the whole datasets. For each cycle of each trial, the correlation between the AO-based estimation and the actual signal was computed as a function of the time-averaged AO error $\bar{\epsilon}$. The logistic function was then fitted to this data cloud using a least-squares method (Fig. 4).

Note that the value of the correlation may be negative (when the AO-based estimate is poor), but not the logistic function. This forces the logistic function to remain close to 0 for negative correlations. This behavior is desired when the correlation is close to 0 or negative, CLME should be preferred over AO. The values for the best-fit parameters are: $\lambda = 0.82$ and $\epsilon_{0.5} = 6.2\,\mathrm{deg}$ for the position estimate, and $\lambda = 0.96$ and $\epsilon_{0.5} = 4.6\,\mathrm{deg}$ for the velocity estimate. Note that the transition from CLME to AO is steeper for velocity estimation and occurs for a smaller value of ϵ_{MA}.

VI. Kinematic Estimation Results

Fig. 5 provides a typical estimation result obtained with CLME, using both individualized and generic gains. The individualized CLME produces a good estimation for the position. It is less performant for velocity as it cannot capture all signal variations. The generic CLME performs similarly well, but with a significant offset in its position estimation.

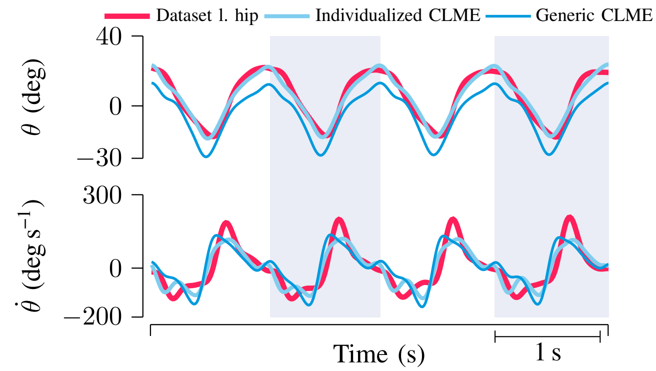

Fig. 5. Time evolution of the left hip angular position (top) and velocity (bottom) from subject 08 walking at $1.2\,\mathrm{m\,s^{-1}}$ (first four cycles). Red lines are taken from [26], light blue lines are the estimates from the individualized CLME and dark blue lines from the generic CLME. Different shades of grey in the background separate successive cycles.

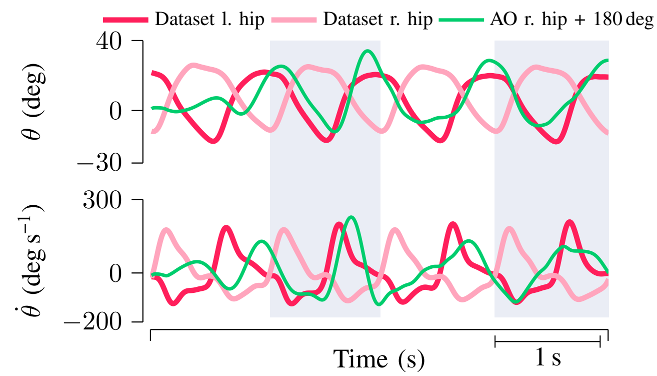

Fig. 6. Time evolution of both hips angular position (top) and velocity (bottom) from subject 08 walking at $1.2\,\mathrm{m\,s^{-1}}$ (first four cycles). Red lines are taken from [26], green lines are estimations from AO. Different shades of grey in the background separate successive cycles.

The same trial is used as a typical trial for AO (Fig. 6). It clearly shows that AO need time to converge to their best estimate, since their quality improves over time. In fact, AO cannot estimate the left leg position well in the first cycle. During the following cycles, the shape and amplitude of the signal converge to those of the actual signals. The estimation convergence is similar for position and velocity.

An example of the fused estimator is depicted in Fig. 7. It is compared to the CLME- and AO-based estiamtors for the same trial as above. Initially, the fused estimator follows the CLME estimation. As ϵ_{MA} decreases, the weight given to AO, W, increases. The AO contributions are not the same for position and velocity, with velocity using more of the CLME estimation. Importantly, the error of the fused estimator is never larger than the largest error of either the CLME- or AO-only estimates. This highlights the interest of the proposed fusion technique, which exploits both approaches during their most favorable epochs.

Finally, we performed a global analysis of all trials com-

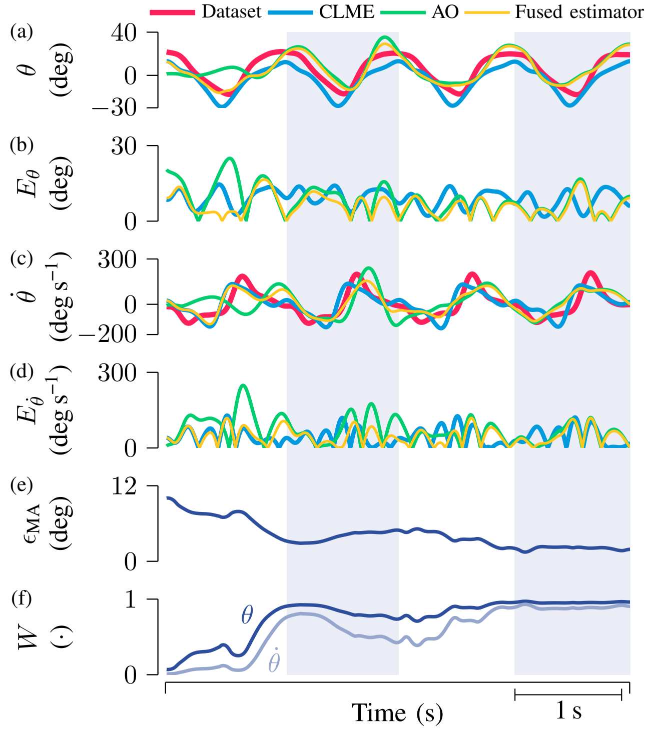

Fig. 7. Time evolution of left hip angular position (a) and velocity (c) from subject 08 walking at $1.2\,\mathrm{m\,s^{-1}}$ (first four cycles). The different lines represent actual data from [26] (red), estimation from CLME after Kalman filter (blue), estimation from AO (green), and estimation from fused estimator (yellow). The position and velocity errors are given in panels (b) and (d), respectively. The evolution of the window-averaged mean error of the AO is given in panel (e), and the corresponding weights of AO in panel (f). Different shades of grey in the background separate successive cycles.

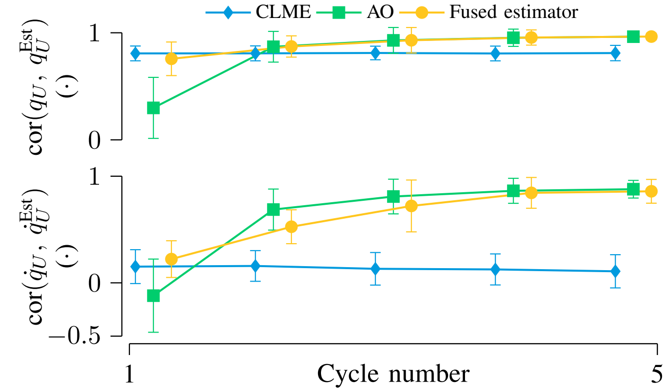

Fig. 8. Correlation between the ground-truth kinematic signals from the datasets and the corresponding estimation provided by the three estimators: CLME only, AO only, and fused one. Values are given for the first five cycles of each trials. Error bars capture the inter-trials standard deviation.

paring the correlation between each of the three estimators (CLME only, AO only, fused) over each cycle and the actual kinematic signals from the whole dataset (Fig. 8). We decided to focus on the first five cycles of each trial, as this is the epoch where the transition between both estimators is most valuable. As expected, CLME provides consistent estimates across cycles for both position and velocity, given that it is time-invariant. Also, the position correlation is higher than the velocity correlation, i.e. about 0.81 for position as compared to 0.14 for velocity. AO obey a dynamic learning trend: their performance is poor during the first cycle, and improves together with their convergence (correlation of about 0.30 in position, and even negative in velocity). They eventually reach a correlation of 0.96 in position and 0.86 in velocity, indicating that they provide a high quality estimate after convergence. As captured by the inter-trial standard deviation, the variability of the AO-based estimate also decreases over time. This variability is equal to 0.28 for the first cycle, and decreases to 0.03 for the fifth one. The fused estimator starts with a performance close to the CLME estimator, and then shifts towards the AO. This holds for both mean and standard deviation.

VII. Conclusion and Discussion

This paper presents a novel method to predict the kinematics of missing leg joint(s) based on corresponding kinematic signals measured on the other leg. The method is designed for both steady-state walking and task transitions, and is based on two estimators of kinematic signals: CLME, a correlation-based approach that works during both transients and steady-state locomotion, and AO, which exploits the rhythmicity of the task and therefore works only during steady-state epochs. First, both methods were presented, and then the fusion approach was explained. We applied the fused estimator to estimate hip kinematic signals from two different datasets. The parameters of the different estimators were computed in a way that they could be used for a generalized population, although this brought some issues for the CLME-based estimation, especially with respect to the position offset. As expected, our new method takes the best of both individual approaches, favoring CLME when AO have not yet converged, and AO otherwise.

We observed that CLME is not robust to position offset. This is expected since its gains are computed on normalized data. Note that this does not degrade the performance metric shown in Fig. 8, i.e. correlation, since it is not sensitive to offset. However, poor offset estimation would be critical in an actual application, such as controlling an orthosis or prosthesis. In our future work, we will investigate the possibility of using the offset estimated by AO, i.e. the state variable α_0, to mitigate this error in the CLME-based estimator, even when AO have not yet converged. Indeed, preliminary results suggest that α_0 converges faster than the other AO state variables.

In the present paper, the performance of our estimator is evaluated only during steady-state walking. However, our method is also designed to handle sharp transients as well. During transitions, e.g. between standing still and walking, we would expect CLME to quickly supersede AO, since the AO error would increase rapidly. Other datasets include such transitions (e.g. [28]) and could be used to assess our method. Preliminary results indicate a good correlation between the CLME-based estimation and the hip signal during such transitions, as well as for other transitions, such as from walking to standing and between different walking speeds. The correlation analysis showed that the contribution of the CLME to our fused estimator is larger in the first cycle, where the convergence of the AO is low. Effective control of powered devices requires accurate estimation for each cycle, including the very first one, thus highlighting the necessary contribution of CLME in our method, even if limited to few cycles. Moreover, we expect that locomotion in an ecological environment – i.e. out of the treadmill – would contain much more walking speed variations and transitions between tasks, thus providing a larger role to the CLME.

Our newly developed method is well suited for real-time applications, since neither CLME nor AO require large computational power. Instead, both rely on a minimal amount of code. Furthermore, input signals can be acquired in real-time, for example using IMUs.

Our future work will focus in implementing the proposed estimator for the control of our designed hip prosthesis [11] and evaluating its performance in generating reference signals for this device.

References

[1] Y. Fang and Z. F. Lerner, "Bilateral vs. Paretic-Limb-Only Ankle Exoskeleton Assistance for Improving Hemiparetic Gait: A Case Series," *IEEE Robot. Autom. Lett.*, vol. 7, no. 2, pp. 1246–1253, Apr. 2022. DOI:10.1109/lra.2021.3139540

[2] B. Kalita, J. Narayan, and S. K. Dwivedy, "Development of Active Lower Limb Robotic-Based Orthosis and Exoskeleton Devices: A Systematic Review," *Int J of Soc Robotics*, vol. 13, no. 4, pp. 775–793, July 2021. DOI:10.1007/s12369-020-00662-9

[3] F. Heremans, J. Evrard, D. Langlois, and R. Ronsse, "A Lightweight and Compact Lockable Parallel Spring Enhances the Performance of a Powered Ankle-Foot Prosthesis," in *2024 10th IEEE RAS/EMBS International Conference for Biomedical Robotics and Biomechatronics (BioRob)*, Sept. 2024, pp. 407–412. DOI:10.1109/biorob60516.2024.10719808

[4] I. Fagioli, A. Mazzarini, C. Livolsi, E. Gruppioni, N. Vitiello, S. Crea, and E. Trigili, "Advancements and Challenges in the Development of Robotic Lower Limb Prostheses: A Systematic Review," *IEEE Transactions on Medical Robotics and Bionics*, vol. 6, no. 4, pp. 1409–1422, Nov. 2024. DOI:10.1109/tmrb.2024.3464126

[5] H. Laloyaux and R. Ronsse, "Extraction of simple monophasic motor primitives towards bio-inspired locomotion assistance," in *2019 IEEE International Conference on Cyborg and Bionic Systems (CBS)*, Sept. 2019, pp. 253–260. DOI:10.1109/cbs46900.2019.9114458

[6] T. K. Best, K. R. Embry, E. J. Rouse, and R. D. Gregg, "Phase-Variable Control of a Powered Knee-Ankle Prosthesis over Continuously Varying Speeds and Inclines," in *2021 IEEE/RSJ International Conference on Intelligent Robots and Systems (IROS)*, Sept. 2021, pp. 6182–6189. DOI:10.1109/iros51168.2021.9636180

[7] A. Mohammadi and R. D. Gregg, "Variable Impedance Control of Powered Knee Prostheses Using Human-Inspired Algebraic Curves," *Journal of Computational and Nonlinear Dynamics*, vol. 14, no. 101007, Sept. 2019. DOI:10.1115/1.4043002

[8] S. K. Au, J. Weber, and H. Herr, "Powered Ankle–Foot Prosthesis Improves Walking Metabolic Economy," *IEEE Trans. Robot.*, vol. 25, no. 1, pp. 51–66, Feb. 2009. DOI:10.1109/tro.2008.2008747

[9] T. K. Best, C. G. Welker, E. J. Rouse, and R. D. Gregg, "Data-Driven Variable Impedance Control of a Powered Knee–Ankle Prosthesis for Adaptive Speed and Incline Walking," *IEEE Transactions on Robotics*, vol. 39, no. 3, pp. 2151–2169, June 2023. DOI:10.1109/tro.2022.3226887

[10] F. Dzeladini, J. van den Kieboom, and A. Ijspeert, "The contribution of a central pattern generator in a reflex-based neuromuscular model," *Front Hum Neurosci*, vol. 8, p. 371, 2014. DOI:10.3389/fnhum.2014.00371

[11] L. Devillez, B. Herman, and R. Ronsse, "Design of a Compact Active Hip Prosthesis with Human-Like Range of Motion and Torque," in *2024 10th IEEE RAS/EMBS International Conference for Biomedical Robotics and Biomechatronics (BioRob)*, Sept. 2024, pp. 160–166. DOI:10.1109/biorob60516.2024.10719919

[12] N. Hogan and D. Sternad, "Dynamic primitives in the control of locomotion," *Front. Comput. Neurosci.*, vol. 7, June 2013. DOI:10.3389/fncom.2013.00071

[13] M. R. Tucker, J. Olivier, A. Pagel, H. Bleuler, M. Bouri, O. Lambercy, J. d. R. Millán, R. Riener, H. Vallery, and R. Gassert, "Control strategies for active lower extremity prosthetics and orthotics: A review," *Journal of NeuroEngineering and Rehabilitation*, vol. 12, no. 1, p. 1, Jan. 2015. DOI:10.1186/1743-0003-12-1

[14] A. H. Hansen and D. S. Childress, "Investigations of roll-over shape: Implications for design, alignment, and evaluation of ankle-foot prostheses and orthoses," *Disability and Rehabilitation*, vol. 32, no. 26, pp. 2201–2209, Jan. 2010. DOI:10.3109/09638288.2010.502586

[15] W. J. Wang, J. Li, W. D. Li, and L. N. Sun, "An Echo-Based Gait Phase Determination Method of Lower Limb Prosthesis," *Advanced Materials Research*, vol. 706–708, pp. 629–634, 2013. DOI:10.4028/www.scientific.net/amr.706-708.629

[16] R. Ronsse, S. M. M. De Rossi, N. Vitiello, T. Lenzi, M. C. Carrozza, and A. J. Ijspeert, "Real-Time Estimate of Velocity and Acceleration of Quasi-Periodic Signals Using Adaptive Oscillators," *IEEE Trans. Robot.*, vol. 29, no. 3, pp. 783–791, June 2013. DOI:10.1109/tro.2013.2240173

[17] H. Vallery and M. Buss, "Complementary limb motion estimation based on interjoint coordination using Principal Components Analysis," in *2006 IEEE International Conference on Control Applications*, Oct. 2006, pp. 933–938. DOI:10.1109/cacsd-cca-isic.2006.4776770

[18] H. Vallery, R. Ekkelenkamp, M. Buss, and H. van der Kooij, "Complementary Limb Motion Estimation based on Interjoint Coordination: Experimental Evaluation," in *2007 IEEE 10th International Conference on Rehabilitation Robotics*, June 2007, pp. 798–803. DOI:10.1109/icorr.2007.4428516

[19] H. Vallery, E. H. F. van Asseldonk, M. Buss, and H. van der Kooij, "Reference Trajectory Generation for Rehabilitation Robots: Complementary Limb Motion Estimation," *IEEE Trans. Neural Syst. Rehabil. Eng.*, vol. 17, no. 1, pp. 23–30, Feb. 2009. DOI:10.1109/tnsre.2008.2008278

[20] H. Vallery, R. Burgkart, C. Hartmann, J. Mitternacht, R. Riener, and M. Buss, "Complementary limb motion estimation for the control of active knee prostheses," *Biomedical Engineering / Biomedizinische Technik*, vol. 56, no. 1, pp. 45–51, Feb. 2011. DOI:10.1515/bmt.2010.057

[21] N. St-Onge and A. G. Feldman, "Interjoint coordination in lower limbs during different movements in humans," *Exp Brain Res*, vol. 148, no. 2, pp. 139–149, Jan. 2003. DOI:10.1007/s00221-002-1212-8

[22] A. Kiffe, C. Graf, and J. Maas, "Feed forward control concept for electric drives," in *2012 IEEE/ASME (AIM)*, July 2012, pp. 332–337. DOI:10.1109/aim.2012.6266046

[23] D. Simon, *Optimal State Estimation: Kalman, H Infinity, and Nonlinear Approaches*. John Wiley & Sons, June 2006.

[24] A. Kelly, "A 3D State Space Formulation of a Navigation Kalman Filter for Autonomous Vehicles:," Defense Technical Information Center, Fort Belvoir, VA, Tech. Rep., May 1994. http://www.dtic.mil/docs/citations/ADA282853

[25] L. Righetti, J. Buchli, and A. J. Ijspeert, "Dynamic Hebbian learning in adaptive frequency oscillators," *Physica D: Nonlinear Phenomena*, vol. 216, no. 2, pp. 269–281, Apr. 2006. DOI:10.1016/j.physd.2006.02.009

[26] K. Scherpereel, D. Molinaro, O. Inan, M. Shepherd, and A. Young, "A human lower-limb biomechanics and wearable sensors dataset during cyclic and non-cyclic activities," *Sci Data*, vol. 10, no. 1, p. 924, Dec. 2023. DOI:10.1038/s41597-023-02840-6

[27] J. Camargo, A. Ramanathan, W. Flanagan, and A. Young, "A comprehensive, open-source dataset of lower limb biomechanics in multiple conditions of stairs, ramps, and level-ground ambulation and transitions," *Journal of Biomechanics*, vol. 119, p. 110320, Apr. 2021. DOI:10.1016/j.jbiomech.2021.110320

[28] A. Sharma, V. Rai, M. Calvert, Z. Dai, Z. Guo, D. Boe, and E. Rombokas, "A Non-Laboratory Gait Dataset of Full Body Kinematics and Egocentric Vision," *Sci Data*, vol. 10, p. 26, Jan. 2023. DOI:10.1038/s41597-023-01932-7